Available online at www.sciencedirect.com
SCIENCE DIRECT®
Developmental Biology 269 (2004) 183–195
DEVELOPMENTAL BIOLOGY
www.elsevier.com/locate/ydbio

Cell cycle-dependent expression of a *hairy* and *Enhancer of split* (*hes*) homolog during cleavage and segmentation in leech embryos

Mi Hye Song,[1] Françoise Z. Huang, Foster C. Gonsalves, and David A. Weisblat*

Department of Molecular and Cell Biology, University of California, Berkeley, CA 94720-3200, USA

Received for publication 14 November 2003, revised 20 January 2004, accepted 20 January 2004

Abstract

We have cloned genes related to *hairy* and *Enhancer of split* (*hes*) from glossiphoniid leeches, *Helobdella robusta* and *Theromyzon rude*. In leech, segments arise sequentially in anteroposterior progression from a posterior growth zone that consists of five bilaterally paired embryonic stem cells called teloblasts. Each teloblast gives rise to segmental founder cells (primary blast cells) that contribute iterated sets of definitive progeny in each segment. Thus, in leech, the "segmentation clock," is closely identified with the cell cycle clock of the teloblasts. We have characterized normal expression patterns of mRNA and protein for the *H. robusta hes*-class gene (*Hro-hes*). Semiquantitative RT-PCR revealed that *Hro-hes* mRNA levels peak while the teloblasts are actively producing primary blast cells. RT-PCR, in situ hybridization and immunostaining revealed that *Hro-hes* is expressed as early as the first zygotic mitosis and throughout early development. *Hro-hes* is expressed in macromeres, pro-teloblasts, teloblasts and primary blast cells. HRO-HES protein is localized in the nuclei of cells expressing HRO-HES during interphase; nuclear HRO-HES is reduced during mitosis. In contrast, *Hro-hes* is transcribed during mitosis and its transcripts are associated with mitotic apparatus (MA). Thus, *Hro-hes* transcription cycles in antiphase to the nuclear localization of HRO-HES protein. These results indicate that *Hro-hes* expression, and thus possibly its biological activity, is linked to the cell cycle.

Keywords: Leech; Segmentation; *hes*; Lophotrochozoa; *Helobdella*; Cell cycle

Introduction

The *Drosophila* gene *hairy* encodes a bHLH transcription factor that functions as a primary pair rule gene in establishing segmental primordia (Carroll et al., 1988; Hooper et al., 1989; Ingham, 1985; Nusslein-Volhard and Wieschaus, 1980) and as a negative regulator of proneural genes in the imaginal disks (Ohsako et al., 1994). *Enhancer of split* is a structurally related gene required for cell fate specification in the peripheral nervous system in *Drosophila* (Knust et al., 1987). *hairy* and *Enhancer of split* (*hes*)-related genes are expressed in the posterior growth zones of sequentially segmenting arthropods (short- and intermediate-germ insects, spiders) and often in stripes just anterior to the posterior growth zone (Damen et al., 2000; Sommer and Tautz, 1993).

Vertebrate *hes*-gene families have been identified, and some family members have been shown to participate in the biochemical oscillations that comprise the "segmentation clock" in the presomitic mesoderm (PSM) and somites of vertebrates (Bessho et al., 2001; Holley et al., 2000; Hirata et al., 2002; Jouve et al., 2000; Muller et al., 1996; Oates and Ho, 2002; Palmeirim et al., 1997; reviewed by Pourquie, 2001a,b; Lewis, 2003). The similarities in expression of *hes*-class genes among vertebrate and basal arthropods have suggested to some that the last common ancestor of protostomes and deuterostomes was already segmented (De Robertis, 1997; Kimmel, 1996).

On the other hand, recent molecular phylogenies suggest that most bilaterally symmetric animals fall into three superphyla, Deuterostomia, Ecdysozoa and Lophotrochozoa (Aguinaldo et al., 1997; Collins and Valentine, 2001; Ruiz-Trillo et al., 1999), which were already separated from

* Corresponding author. Department of Molecular and Cell Biology, University of California, 385 LSA, Berkeley, CA 94720-3200. Fax: +1-510-643-6791.
E-mail address: weisblat@berkeley.edu (D.A. Weisblat).
[1] Present address: Department of Molecular, Cellular and Developmental Biology, University of Michigan, Ann Arbor, MI 48109-1048.

0012-1606/$ - see front matter © 2004 Published by Elsevier Inc.
doi:10.1016/j.ydbio.2004.01.025

one another at the time of the Cambrian radiation (Adoutte et al., 2000). Most groups in each of these superphyla are unsegmented. Thus, parsimony favors the notion that segmentation has arisen independently in Deuterostomia (vertebrates), Ecdysozoa (arthropods, onychophorans, tardigrades) and Lophotrochozoa (annelids, including leeches). Comparative studies including segmented and unsegmented taxa in all three superphyla should further our understanding of segmentation mechanisms and the evolution of segmentation.

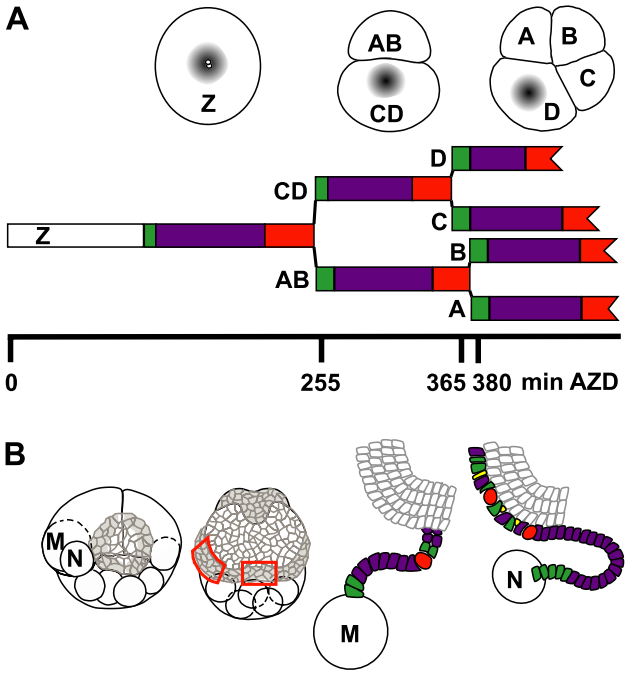

Fig. 1. Relevant aspects of *Helobdella* development. (A) Animal pole views of one-, two- and four-cell embryos (top), and corresponding differences in cell cycle duration and composition (bottom). Zygotes (Z) remain in meiotic arrest until they are laid, so developmental times are indicated as minutes after zygote deposition (AZD). Cytoplasmic rearrangements during the first cell cycle yield pools of yolk-free cytoplasm (teloplasm; shading) that segregate to the D lineage. (B) During cleavage, five bilateral pairs of segmentation stem cells (teloblasts) arise from the D quadrant. Left-hand M and N teloblasts are indicated in a stage 7 embryo (left, approximately 55 h AZD); M (mesodermal) and N (one of 4 ectodermal) teloblasts are labeled on the left side. Teloblasts generate coherent bandlets of segmental founder cells (blast cells) that coalesce to form left and right germinal bands (gray shading), beneath a micromere-derived epithelium (indicated by irregular small contours). Red boxes on the mid-stage 8 embryo (center, approximately 65 h AZD) correspond to the views shown in Figs. 5I and J. Drawings at right depict isolated M_L and N_L teloblasts and their blast cell progeny, color-coded to depict their progression through the cell cycle. Note that the m blast cells divide before entering the germinal band (the ectodermal bandlets are indicated in gray), whereas the two classes of n blast cells divide after they are already within the germinal band (o, p and q bandlets are indicated in gray). Cell cycle coding: meiosis, white; G1 phase, yellow; S phase, green; G2 phase, purple; mitosis, red. Note that early cell cycles (panel A) contain no G1 phase; G1 is first seen in small progeny arising from unequal divisions of primary blast cells (N lineage in panel B).

Toward that end, we have identified *hes*-class genes (*Tru-hes* and *Hro-hes*) from two glossiphoniid leeches, *Theromyzon rude* and *Helobdella robusta*, respectively. Embryos of leeches (and other clitellate annelids) generate segments via stereotyped cell lineages (Fig. 1; Shankland, 1999), so that in this group, there is a strict correlation between the "segmentation clock" and the cell cycle clock, in contrast to vertebrates and many arthropods. A key feature of this process is the production of segmental founder cells (blast cells) in anteroposterior progression from a set of 10 identified stem cells (teloblasts) that constitute a posterior growth zone (Fig. 1). In glossiphoniid leeches such as *Helobdella*, the teloblasts are large and experimentally accessible.

Semiquantitative RT-PCR revealed that mRNA expression of *Hro-hes* peaks during the period when teloblasts are making blast cells (Fig. 1). In situ hybridization and immunostaining revealed that *Hro-hes* is expressed throughout cleavage and early development in a variety of cell types, including teloblasts and primary blast cells. Immunostaining shows that HRO-HES is localized in nuclei during interphase but declines or is diluted throughout the cytoplasm during mitosis, whereas in situ hybridization shows that *Hro-hes* transcripts are associated with the mitotic apparatus of dividing cells. Inhibitor studies coupled with in situ hybridization, and RT-PCR on individually staged zygotes reveal that *Hro-hes* is transcribed during mitosis. Thus, *Hro-hes* transcripts and HRO-HES protein exhibit reciprocal nuclear localization during the cell cycle in early development. These results show that expression of this *hes*-class gene in leech (superphylum Lophotrochozoa) is linked to the cell cycle in a manner that has not been described for the various *hes*-class genes examined in representatives of Deuterostomia or Ecdysozoa.

Materials and methods

Embryos

Embryos of *H. robusta* and *T. rude* were obtained and cultured in *Helobdella* (HL) saline as described in Song et al. (2002). The embryonic staging system and cell nomenclature are as summarized elsewhere (Weisblat and Huang, 2001). To label particular cell lines, cells of interest were pressure-injected with rhodamine- or fluorescein-conjugated dextran amine (RDA or FDA) as described previously (Smith and Weisblat, 1994).

To block RNA synthesis, embryos were bathed in actinomycin-D mannitol (Sigma), 100–500 μg/ml in HL saline for 2–5 h at room temperature. In some experiments, the incubation medium for both experimental and control embryos included 0.5% dimethyl sulfoxide (DMSO; Sigma) to accelerate the penetration of the drug into the embryos.

Gene cloning

Candidate gene fragments were amplified from genomic DNA by degenerate PCR. Degenerate oligonucleotides (upstream = 5′-MGIGCIMGIATIAAYRAITSIYT-3′; downstream = 5′-ACIGTYWTYTCIARIATITCIGCYTT-3′) were designed by comparing the bHLH domains of the *hes*-class genes from *Drosophila melanogaster* and *D. virilis* (Bier et al., 1992; Rushlow et al., 1989), rat (Feder et al., 1993), human (Feder et al., 1994) *Tribolium castaneum* (Sommer and Tautz, 1993) and frog (Dawson et al., 1995). Additional sequence was obtained by 5′- and 3′-RACE on first-strand cDNAs and on a cDNA library prepared commercially (Stratagene) from stages 7–10 embryos and from further PCR from genomic DNA.

Semiquantitative developmental RT-PCR

Fifty embryos from each stage were collected and processed as in Song et al. (2002). To confirm the relative levels of expression, we amplified two separate regions of *Hro-hes* cDNA: nt 162–470 (which spans an intron site, to control for genomic DNA contamination of the template) and nt 960–1133. The *Hro-hes* fragments were amplified using the following PCR cycles: 1 min at 94°C, 1 min at 60°C and 30 s at 72°C for 5 cycles; followed by 1 min at 95°C, 1 min at 58°C and 30 s at 72°C for 30 cycles. The two primer sets gave equivalent results and one sample of each fragment was sequenced to confirm the identity of the amplified PCR products.

Single zygote RT-PCR

Freshly laid zygotes were timed relative to the appearance of the second polar body, defined as 105 min after zygote deposition (AZD). Individual zygotes were lysed at selected time points in 10 μl cell lysis buffer (Cells-to-cDNA kit, Ambion Inc.) by heating at 75°C for 5 min. DNA was digested by the addition of 1 U DNAse (Ambion Inc.), followed by incubation at 37°C for 30 min. DNAse was then inactivated by heating at 75°C for 5 min. Reverse transcription (RT) was carried out on 9.5 μl of the zygotic lysate using random decamers (Ambion Inc.) and 100 U Superscript Reverse Transcriptase II (Invitrogen Inc.) using reaction conditions as described by manufacturer. RT was allowed to proceed for 1 h at 42°C. PCR for *Hro-hes* was performed using the same primers (spanning nt 162–470) and amplification conditions as for the developmental RT-PCR described above, except using 3 $MgCl_2$. To increase the sensitivity of the procedure, a second round of amplification was carried out, using the same conditions, starting with 5 μl of the primary PCR as the template. A maternal transcript, *Hro-nanos* cDNA was also amplified as a positive control using gene specific primers (Kang et al., 2002; Pilon and Weisblat, 1997). Amplicons were resolved on a 2% agarose gel. The gels were blotted and processed for Southern hybridization (Sambrook et al., 1989), then probed with a ^{32}P-labeled DNA probe spanning nt 185–445 of *Hro-hes* and exposed to X-ray film at −80°C for various intervals.

In situ hybridization

Digoxygenin (Dig-11-UTP, Roche)-labeled riboprobes were made in vitro (MEGAscript kit, Ambion Inc.). T7 RNA polymerase (Ambion Inc.) was used to transcribe both sense and antisense probes. Hydrolyzed and unhydrolyzed probe produced equivalent staining patterns. To further confirm the in situ patterns, we carried out in situ staining with two different probes for *Hro-hes*, one from nt 1 to 1133 containing both intron sequences and the bHLH domain, and the other from nt 676 to 1779 encoding C-terminal amino acids and 3′-UTR. Both probes generated the same patterns. In situ hybridization was performed as described in Song et al. (2002).

Recombinant protein expression and antibody production

To generate polypeptides for antibody production, portions of *Hro-hes* were selected from the coding region (nt 678–1132) that excluded the bHLH domain and the asparagine-rich region to avoid cross reactivity. This fragment was cloned into pQE-30 expression vector (Qiagen) for producing N-terminal 6× His-tagged polypeptide. The affinity-purified antibody against *Hro-hes* antigen was prepared as described previously (Goldstein et al., 2001).

Immunostaining

Embryos were fixed with 4% formaldehyde in 0.25× phosphate-buffered saline (PBS, diluted from 10× stock) for 1 h at RT. Embryos were washed in PBS with 1% Tween-20 (PBTw), devitellinized and incubated for 3 h in a solution of 10% normal goat serum in PBTw (PTN), then in the antibody of *Hro-hes* (anti-HRO-HES, 1:1000) in PTN at 4°C for 2 days. All incubations and subsequent washes were done with constant agitation. After washing with frequent changes of PBTw at RT for 5 h, embryos were incubated in a peroxidase-conjugated goat anti-rabbit IgG (Jackson Lab, 1:1000) in PTN at 4°C for 2 days, then washed in PBTw and incubated with 0.5 mg/ml diaminobenzidine in PBS and 0.003% H_2O_2 for color reaction. For zygotes, 1% Triton X-100 was substituted for 1% Tween-20 and also antibody incubation were done overnight at RT, instead of 2 days at 4°C.

To double label for histone and HRO-HES, histone antibody (Chemicon, 1:1000) and Alexa 488 goat anti-mouse IgG (H + L) (Molecular Probes, 1:1000) were included in the primary and secondary antibody incubations, respectively. After color development, embryos were rinsed with PBS, dehydrated, cleared in benzyl benzoate/benzyl alcohol (3:2) and examined in whole mount by epifluorescence microscopy (Zeiss Axiophot) and photographed on

35-mm film. Slides were scanned and images were processed digitally (Metamorph, UIC).

Results

Identification of hes-class genes from glossiphoniid leeches

We first amplified genomic fragments of *hes*-class genes from both *H. robusta* and *T. rude*. These fragments encode portions of the bHLH domain of the predicted *hes*-class genes, designated as *Hro-hes* (accession# AY144625) and *Tru-hes* (accession# AY144624). Each fragment contains an intron (126 and 324 bp, respectively) at a site that is conserved with respect to other organisms (Fig. 2). For *Tru-hes*, we obtained only a partial sequence within the bHLH domain. For *Hro-hes*, we identified another intron (125 bp) within the bHLH domain, also as in other organisms (Fig. 2). The bHLH domains of *Hro-hes* and *Tru-hes* are similar, suggesting that we had identified the same subgroup of leech *hes*-class gene in both. (By comparison with other animals, it seems likely that *Helobdella* has more than one *hes*-class gene, but this remains to be determined.) For *Hro-hes*, we used 5′- and 3′-RACE on cDNA libraries and first-strand cDNAs for additional sequence and obtained an ORF encoding 436 amino acids plus 5′-UTR (189 bp) and 3′-UTR (224 bp). Three in-frame stop codons lie upstream of the presumed start codon, suggesting that we obtained the complete ORF of *Hro-hes* (Fig. 2A). The 3′-UTR includes one polyadenylation site and also two sites resembling what has been identified in vertebrates as a cytoplasmic polyadenylation element (CPE; Ryskov et al., 1983; Fig. 2C). Like other *hes*-class genes, *Hro-hes* also contains a version of the C-terminal WRPW motif that is required for *groucho*-dependent repression in *Drosophila* (Aronson et al., 1997). The C-terminal WRPF tetrapeptide in *Hro-hes* matches that of a spider *hes*-class gene (*Cs-H*) (Damen et al., 2000). The bHLH domain of *Hro-hes* is quite divergent, showing only 51% identity with *Drosophila hairy* and 61% identity with chick *c-hairy1* (Fig. 2B). Apart from the bHLH and WRPW domains, we were unable to make reliable alignments between *Hro-hes* and other *hes*-class genes. A phylogram [PAUP 4.0 b4a (PPC)] using only bHLH domains reliably places *Hro-hes* within the class of *hes*-related genes, but offers little regarding the phylogenetic relationships within that group (Fig. 3).

Hro-hes transcript levels peak during production of segmental founder cells

Semiquantitative RT-PCR (Spencer and Christensen, 1999) was used to estimate the relative levels of *Hro-hes* mRNA accumulation during development (see Fig. 1 for description of relevant developmental stages). As an internal control for variations in efficiency of RNA extraction and cDNA synthesis, we also performed submaximal PCR

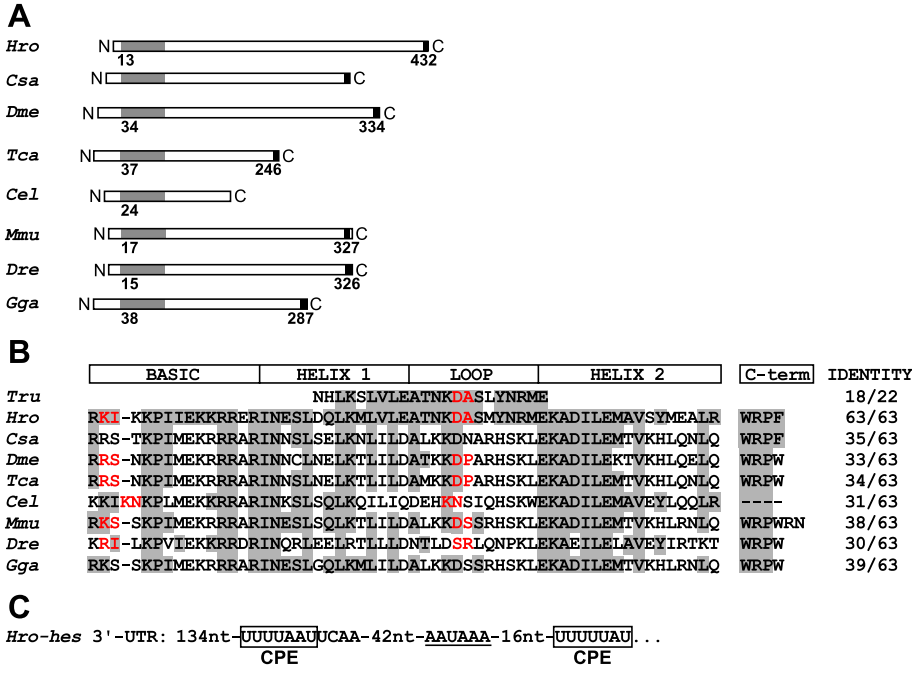

Fig. 2. A *hes*-class gene from *H. robusta*. (A) Comparison of *Hro-hes* and other selected *hes*-class genes showing overall domain structure; numbers indicate the amino acid residue corresponding to the start of the bHLH (gray) and C-terminal (black) domains, where known. (B) Amino acid alignments for the bHLH and C-terminal domains for the proteins in A plus the gene fragment obtained from *T. rude*. Residues identical to those in *Hro-hes* are highlighted; known intron sites are indicated in red. (C) Part of the *Hro-hes* 3′-UTR showing cytoplasmic polyadenylation element (CPE) consensus sites (boxes) and polyadenylation site (underlined). Tru, *Tru-hes* [from *Theromyzon* (leech)]; Hro, *Hro-hes* (leech); Csa, spider *hairy*; Dme, *Drosophila hairy*; Tca, beetle *hairy*; Cel, *lin22* (nematode); Mmu, *hes1* (mouse); Dre, *her1* (zebrafish); Gga, chick *c-hairy1*.

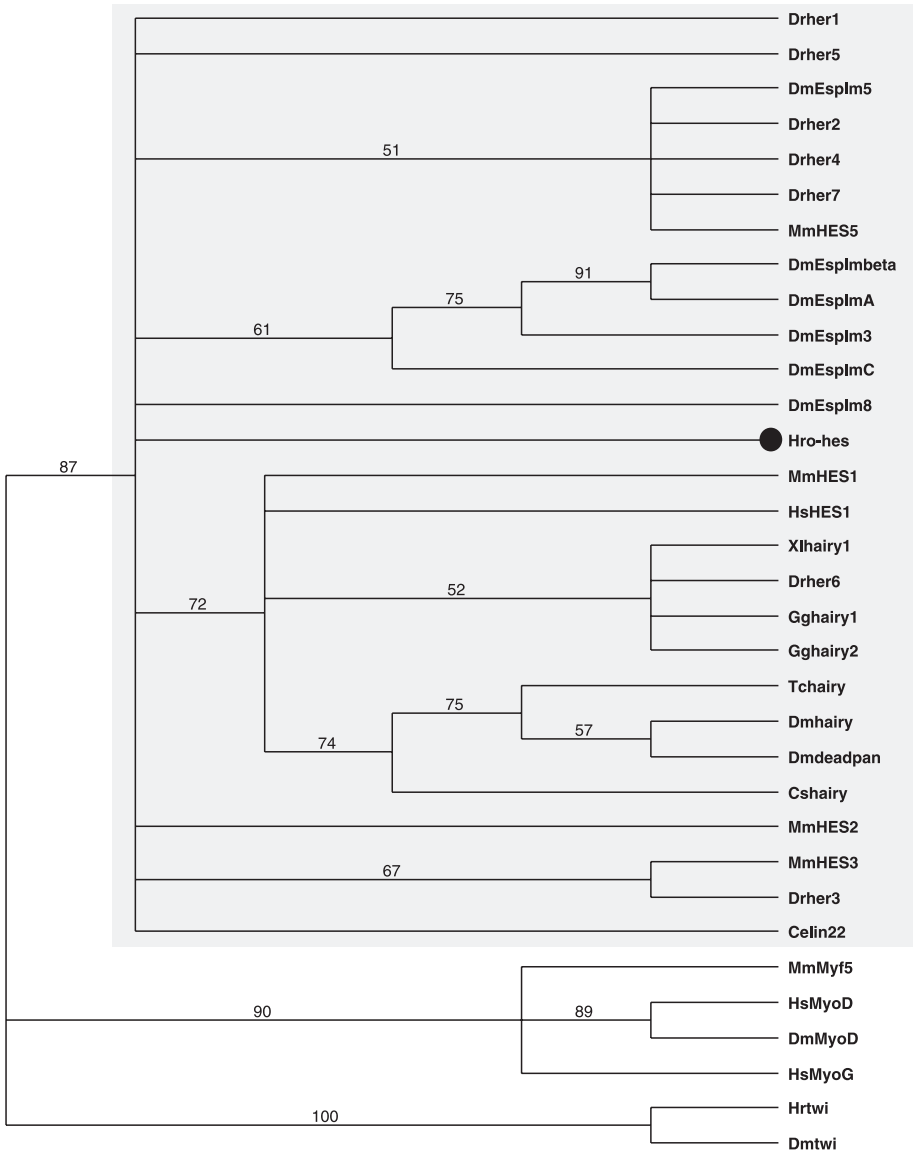

Fig. 3. Phylogram comparing the bHLH domains of selected proteins indicates that *Hro-hes* (black circle) belongs to the *hes* gene family (highlighted). The tree was generated using PAUP*4.0b4a(PPC). Representative *twist*- and *myoD*-related sequences are included as outgroups and are separated by a node with 87% confidence level. All sequences are taken from GenBank. Espl, *enhancer-of-split* genes; HES, *hairy* and *Enhancer of split* genes; her, *hairy* and *enhancer-of-split*-related genes; Dr, *Danio rerio*; Dm, *D. melanogaster*; Mm, *Mus musculus*; Hs, *Homo sapiens*; Xl, *Xenopus laevis*; Gg, *Gallus gallus*; Tc, *T. castaneum*; Ce, *Caenorhabditis elegans*; Cs, *Cupienius salei*.

amplification of 18S rRNA fragments for each stage sampled. The oligos were chosen to span introns in *Hro-hes*, so that PCR fragments arising from genomic DNA contamination could be distinguished by their larger size. To further confirm the relative levels of expression, we amplified two separate regions of *Hro-hes* using two independent pairs of primers, which produced equivalent results.

By this assay, *Hro-hes* mRNA was not detected during cleavage until stage 5 or 6 (approximately 15–20 h AZD; Figs. 1 and 4). Transcript levels peak during stage 7 (approximately 40–50 h AZD) and then decline during stage 8 (60–90 h AZD; Fig. 4). This period of peak expression corresponds to the stage in which the teloblasts are making segmental founder cells.

Immunohistochemical characterization of HRO-HES expression

Attempts to quantify HRO-HES protein expression by developmental Western blot analysis were unsuccessful because of the limited numbers of embryos available. So we characterized HRO-HES expression immunohistochemically (Fig. 5), starting with stages 7 and early 8, in which

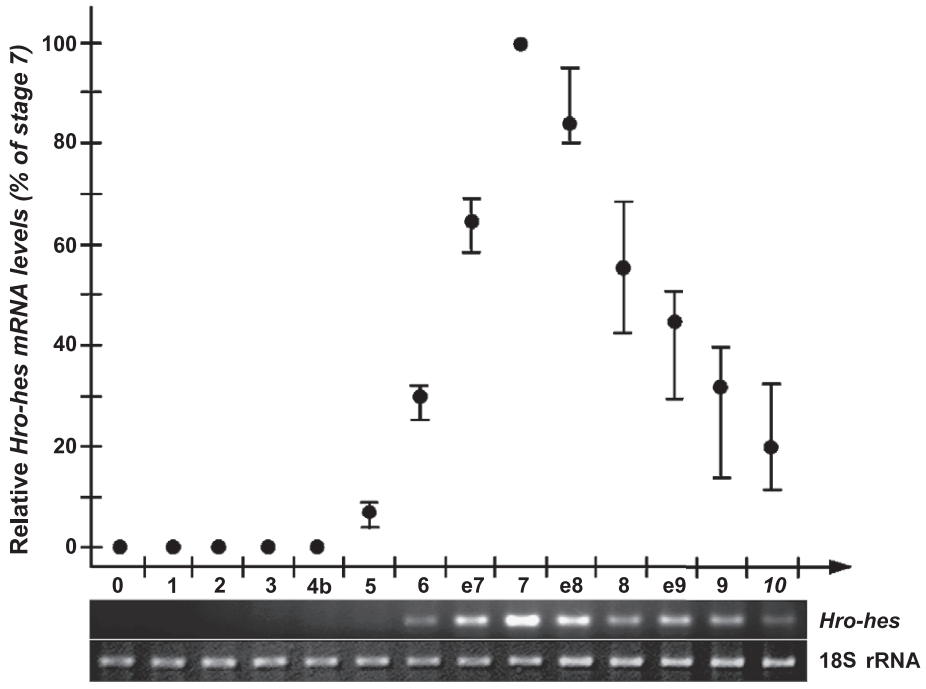

Fig. 4. *Hro-hes* transcript levels peak during teloblast function. Semiquantitative RT-PCR of *Hro-hes* at developmental stages 1–10 (see Fig. 1; stage 0 represents oocytes dissected from gravid adults) using 18S rRNA as an internal control for variations in efficiency of the RNA extraction and cDNA synthesis procedure (see Materials and methods). Ethidium bromide-stained gel (below) shows *Hro-hes* and 18S rRNA bands from the stages indicated. To avoid saturation of amplified PCR products, we performed submaximal PCR amplification (33 amplification cycles for *Hro-hes* and 23 cycles for 18S rRNA). Under these conditions, no transcript was detected during cleavage stages 1–4. The graph (above) shows the average of the intensity of the *Hro-hes* bands after normalizing by the intensity of the corresponding 18S rRNA bands and plotting relative to stage 7 from five different experiments. Error bars indicate the range of values obtained.

strong expression was expected from the RT-PCR results described above. Immunostaining at these stages revealed HRO-HES in nuclei, as expected for a transcription factor. Anti-HRO-HES uniformly labeled most teloblasts and primary blast cells in all lineages (Figs. 5F–I), including supernumerary blast cells that do not contribute progeny to definitive segments. We observed no alternating patterns of HRO-HES expression among primary blast cells or their progeny that might indicate a pair rule function for *Hro-hes* (Figs. 5F–I). Moreover, examination of other embryonic stages revealed anti-HRO-HES staining of interphase nuclei as early as the two-cell stage (Fig. 5C) and including macromeres and micromeres (Figs. 5E, F). Thus, HRO-HES expression is not correlated with decisions as to either cell type or segmental vs. nonsegmental cell fates in the *Helobdella* embryo.

HRO-HES immunostaining of nuclei disappeared or was greatly reduced during mitosis, which is not surprising given the nuclear envelope breakdown during this phase of the cell cycle. The correlation between cell cycle and HRO-HES immunostaining was easily seen in embryos double-stained for HRO-HES (visualized by the DAB reaction) and chromatin (visualized by either a fluorescent DNA stain or anti-histone primary antibody and a fluoresceinated secondary antibody). Chromatin fluorescence was obscured by the DAB reaction product over the nuclei of cells in interphase, but not for those in mitosis (Fig. 5G). Whether the loss of HRO-HES immunostaining during mitosis is solely attributable to its dilution in the cytoplasm upon nuclear envelope breakdown remains to be determined.

As described above, HRO-HES immunostaining of interphase nuclei began as early as the two-cell stage, and there also appeared to be staining above background levels in the teloplasm of the two-cell embryo as well (Figs. 5C, D). No HRO-HES immunostaining above background was observed in the cytoplasm or nucleus of the zygote, however (Figs. 5A, B). This point is critical for experiments in the last part of the Results section.

HRO-HES levels decline as segmental founder cells divide in later development

As described above, the DAB reaction product from HRO-HES immunostaining of nuclei obscured chromatin fluorescence of interphase segmental founder cells (primary blast cells; Figs. 5G, H). In addition to highlighting the cell cycle dependence of the HRO-HES signal, double-staining also revealed a decline in HRO-HES levels as segmental founder cell clones developed. Previous studies have shown that blast cell clones undergo stereotyped division patterns with mitoses at fixed positions relative to the parent teloblast

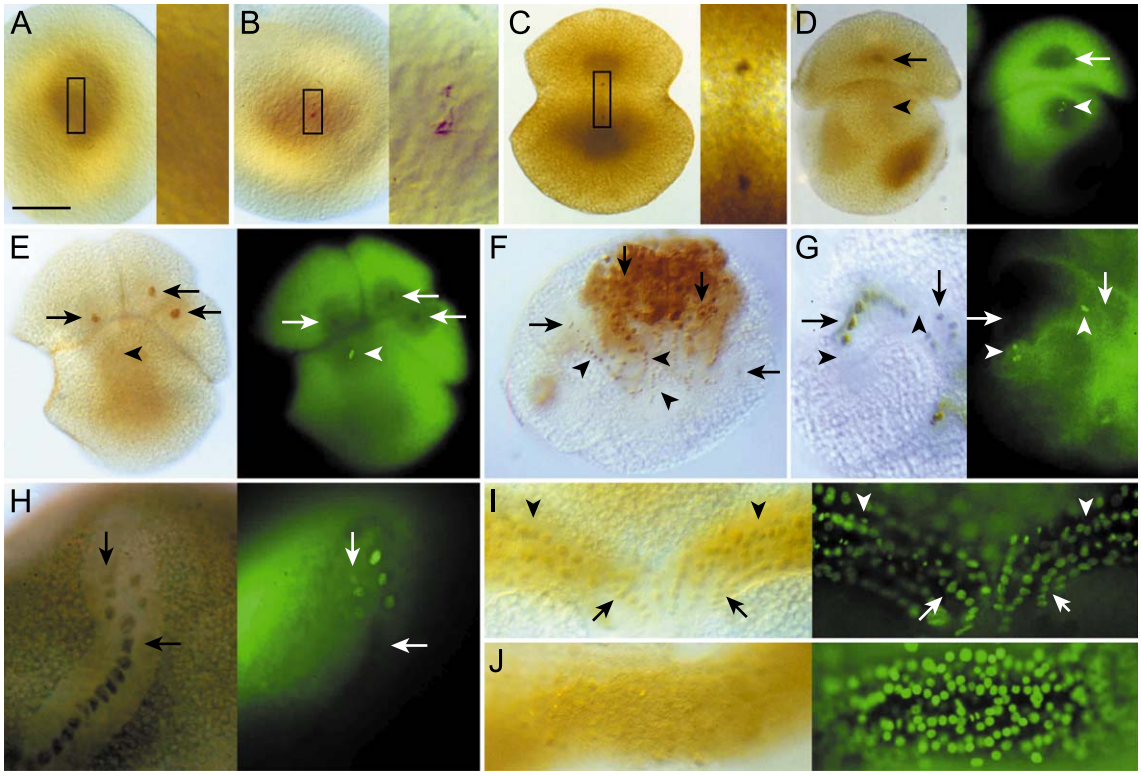

Fig. 5. HRO-HES is expressed beginning in the two-cell stage and through the production of segmental founder cells. (A) Zygote immunostained for HRO-HES (visualized with DAB histochemistry) before first mitosis (approximately 200 min AZD) reveals no detectable nuclear staining. (B) Sibling zygote processed as in (A), but immunostained for histone instead of HRO-HES shows that antibodies were able to penetrate the embryo. (C) Slightly older zygote (250 min AZD) fixed during cytokinesis and processed as in (A); the first mitosis is complete and both interphase nuclei have localized HRO-HES. (Insets at right in (A–C) show nuclear regions at higher magnification). (D) Late two-cell embryo (320 min AZD) double-stained for HRO-HES (left) and histone (right, visualized with a fluoresceinated secondary antibody); cell AB is still in interphase (arrows) and stains for HRO-HES, whereas cell CD has entered mitosis (arrowheads). Note that the DAB reaction product obscures the histone fluorescence in AB (white arrow), but not in CD (white arrowhead). (E) Four-cell embryo (410 min AZD) processed and photographed as in (D); cells A, B and C are in interphase and stain for HRO-HES (arrows), whereas cell D has entered mitosis (arrowheads) and does not. The DAB reaction product obscures the histone fluorescence in A, B and C, but not in D. (F) Stage 7 embryo (approximately 30 h AZD) shows HRO-HES in nuclei of teloblasts (horizontal arrows), blast cells (arrowheads) and micromere derivatives (vertical arrows). (G) Higher magnification view of a similar stage 7 embryo doubled-stained as in (D and E), focusing on the left M teloblast and the column of m blast cells. The DAB reaction product obscures the histone fluorescence in interphase primary blast cells (horizontal arrows) and their progeny (vertical arrows), but not in the M teloblast (horizontal arrowhead) or in the oldest primary blast cell (vertical arrowhead), both of which are in mitosis. (H) An m bandlet from another embryo, immunostained for HRO-HES as above but in this case counterstained with a low-molecular-weight DNA stain (SYTOX Green). Here, the DAB reaction product obscures the DNA fluorescence in the primary blast cells (horizontal arrows), but not in their daughter cells (vertical arrows). (I and J) Close-up views showing portions of the germinal bands of a stage 8 embryo (approximately 65 h AZD) double-stained as in (D and E). In posterior, younger portions of the germinal band (I, see Fig. 1), weak DAB staining indicates the continuing presence of HRO-HES in primary blast cells (arrows) and their progeny (arrowheads), but histone fluorescence breaks through in both interphase and mitotic cells. In more anterior portions of the germinal band, corresponding to older blast cell clones (J, see Fig. 1), nuclear HRO-HES is hardly detected. Scale bar, 100 μm in A–F; 25 μm in insets; 50 μm in G–J.

in each lineage (Bissen and Weisblat, 1989 Zackson, 1984; Fig. 1). In older blast cell clones, the levels of nuclear HRO-HES declined, as judged by the increasing fluorescence breakthrough in interphase nuclei and decreasing intensity of immunostaining in nuclei versus cytoplasm (Figs. 5H–J). This could represent a systematic shift of HRO-HES from nucleus to cytoplasm, but we interpret it as reflecting a decline in HRO-HES levels in older blast cells, consistent with the decline in *Hro-hes* mRNA levels during stage 8 (Fig. 4). Teloblasts gradually cease making primary blast cells during this time (Desjeux and Price, 1999), so if the developing blast cell clones gradually cease expressing *Hro-hes*, it would explain the observation that overall expression levels gradually decline.

Hro-hes transcripts associate with the mitotic apparatus

On the basis of the immunostaining results, we carried out in situ hybridization for *Hro-hes* on embryos at stages 1–8. Consistent with the immunostaining patterns, we detected *Hro-hes* transcripts in blastomeres throughout cleavage and in teloblasts and primary blast cells. Similar to our observations for an *even-skipped*-class gene (*Hro-eve*) in *Helobdella* (Song et al., 2002), we saw no evidence of a pair-rule type pattern of transcription (e.g., periodic variations in expression within the bandlets or germinal bands) for *Hro-hes* (Figs. 6A, B).

Also as for *Hro-eve*, *Hro-hes* transcripts were associated with the mitotic apparatus (MA) of cells undergoing divi-

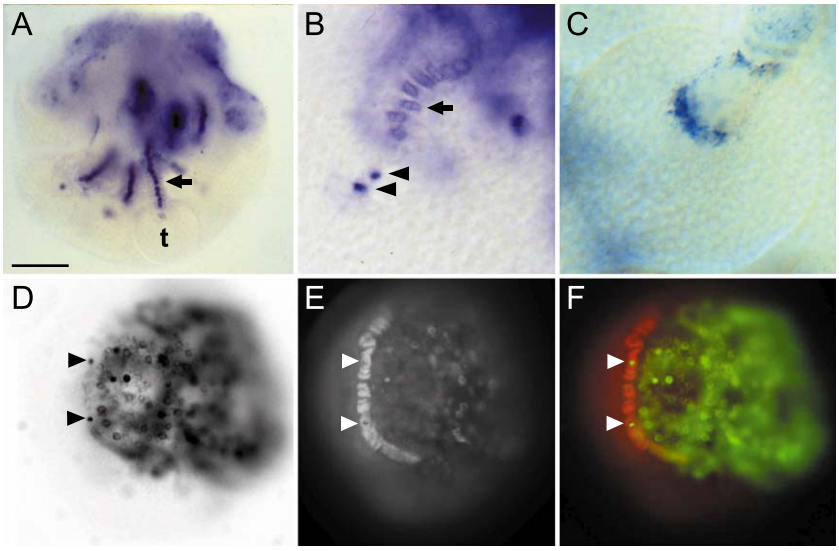

Fig. 6. *Hro-hes* transcripts are associated with mitotic apparatus (MA) of dividing cells. (A) View of a stage 7 embryo processed by in situ hybridization for *Hro-hes*, focused on one of the eight ectodermal teloblasts (t) and its bandlet (arrow). *Hro-hes* staining is perinuclear and uniform within the bandlet; thus, there is no evidence of a "pair-rule" type expression pattern for this gene. (B) A higher magnification view of an embryo similar to that shown in A. In addition to the perinuclear in situ staining evident in the primary blast cells (arrow), note the intense punctate staining associated with the teloblast and the youngest blast cell (arrowheads). We suggest that this staining represents cells that have either just completed mitosis or are in late telophase. (C) View of another stage 7 embryo, comparable to that shown in B, except hybridized with a probe for a cyclin gene, *Hro-cycA*, shows purely cytoplasmic transcript distribution. (D–F) Bright-field, fluorescence and pseudocolored merged views, respectively, of an embryo, processed by in situ hybridization for *Hro-hes* at late stage 7 (approximately 55 h AZD), in which the left N teloblast had been injected with RDA lineage tracer at stage 6a. Punctate staining (arrowheads in D and F) correspond to the sites at which nf (lower arrowheads) and ns (upper arrowheads) blast cells undergo their first mitoses and the stained cells have indeed rounded up for mitosis (arrowheads in E). Scale bar, 100 μm in A, D–F; 40 μm in B and C.

sion, including primary blast cells within the germinal bands (Figs. 6B, D–F). Various criteria allowed us to identify mitotic cells, including the predictable timing of mitoses in precisely staged embryos (Bissen and Weisblat, 1989; Huang et al., 2002; Fig. 1), and the position within the bandlet at which each class of primary blast cells undergoes its first mitosis (Zackson, 1984; Fig. 1). Such cells typically showed an intense, punctate in situ staining pattern for *Hro-hes*.

For example, the columns of primary blast cells produced by the N teloblasts comprise distinct nf and ns blast cells as defined by mitotic pattern and definitive fates (Bissen and Weisblat, 1987, 1989; Weisblat et al., 1984; Zackson, 1984). By labeling an N teloblast with lineage tracer, we were able to observe prominent nuclear in situ signals in two nearby cells in the n bandlet within the germinal band (Figs. 6D, F). The rounded morphology of these cells, as revealed by the RDA lineage tracer, indicated that they were in mitosis and the cells were at the positions where nf and ns blast cells undergo their first mitoses, approximately 26 and 28 h, respectively, after they are born from the N teloblast (Fig. 6E; Bissen and Weisblat, 1989; Zackson, 1984).

As another example, primary m blast cells undergo their first mitoses about 10 h after they are born, which is before their entry into the germinal band. Thus, a dividing primary m blast cell can be identified by its position in the bandlet relative to the teloblast and by its rounded morphology.

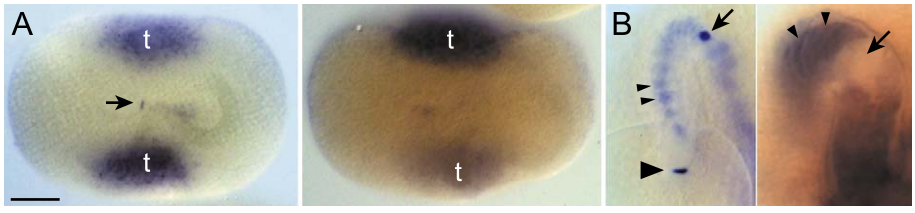

Fig. 7. *Hro-hes* is transcribed during mitosis: actinomycin D blocks in situ staining of MA. Each panel shows a control embryo (left) and a sibling treated with actinomycin D, both processed by in situ hybridization for *Hro-hes*. (A) In control zygotes, *Hro-hes* in situ staining is associated with the MA (arrow) and also gives background staining in teloplasm (t). Embryos treated with actinomycin D divided at the same time as controls (data not shown) but no *Hro-hes* transcripts were detected at the MA. (B) Stage 7 embryos showing in situ staining in the m bandlet at the point where the approximately 10-h old primary blast cells undergo mitosis (left arrow); similar staining is seen in the dividing M teloblast (large arrowhead). This staining is blocked by actinomycin D treatment (right arrow). The actinomycin D-treated embryo at right was overstained to demonstrate the lack of in situ signal in the dividing m blast cell; thus, the cytoplasmic staining in the interphase primary blast cells (small arrowheads; see also Fig. 6) is stronger in the right hand embryo. Scale bar, 100 μm in A; 40 μm in B.

Punctate *Hro-hes* in situ staining was frequently associated with m blast cells at this position (Fig. 7B).

Two different probes for *Hro-hes* (see Materials and methods) were used; both gave the same pattern, although sense probe gave no staining (data not shown). Moreover, probes for *Helobdella* homologs of *cyclinA* (Fig. 6C), *nanos* (data not shown) and *twist* (Ping Xiao, personal communication) gave distinct expression patterns without staining the MA. Thus, the association of *Hro-hes* transcripts with MA is not an artifact of the in situ hybridization protocol.

The severe conditions used for the in situ hybridization were not compatible with simultaneous immunostaining of histones or microtubules, or even DAPI staining for chromatin (data not shown). Thus, although the staining patterns observed were often suggestive of chromatin fixed at different phases of mitosis [e.g., prophase (Figs. 6D, 7B), metaphase (Figs. 7A, B) or telophase (Figs. 6B)], we cannot be sure if the in situ staining is associated with the chromatin or the spindle of the MA, or both.

Hro-hes is transcribed during mitosis: actinomycin D sensitivity of MA staining

One explanation for the association of *Hro-hes* transcripts with the MA of dividing cells is that cytoplasmic transcripts were binding to the MA following nuclear membrane breakdown at the onset of mitosis. Alternatively, it could be that *Hro-hes* was being transcribed during mitosis. To begin to distinguish these possibilities, we carried out in situ hybridization for *Hro-hes* on embryos treated with actinomycin D to inhibit transcription. In one set of experiments, we focused on the easily observed primary m blast cell divisions. Roughly 30% of the m bandlets in control embryos contained punctate in situ staining at the site where the primary m blast cells undergo mitosis. This is in accord with the duration of mitosis (approximately 30 min) relative to the rate at which m blast cells are produced from the M teloblasts in *H. robusta* (one cell per approximately 90 min). Actinomycin D treatment eliminated the punctate in situ staining from the embryo overall, including the primary m blast cells at the site of their first mitosis, without affecting the diffuse staining of adjacent, interphase cells (Fig. 7B).

One interpretation of these results is that *Hro-hes* is transcribed primarily during mitosis, and that the in situ signal in adjacent cells represents the perdurance of the mitotic transcripts during interphase. This interpretation is called into question, however, by the slow onset of the actinomycin D effect; roughly 4-h exposure is required to eliminate the MA staining. This delay may arise in part from the time required for the actinomycin D to reach effective levels within the yolky *Helobdella* embryos. But the delay could also be interpreted to mean that *Hro-hes* is transcribed during interphase, and that the actinomycin D sensitivity of the MA in situ staining reflects a transcriptional requirement for the synthesis of other molecules that stabilize and localize the preexisting *Hro-hes* transcripts to the MA during mitosis.

Hro-hes is transcribed during mitosis: single cell RT-PCR

To examine this issue further, we took advantage of the observations that: (1) in situ staining for *Hro-hes* labels the MA during the first zygotic mitosis (Fig. 7A); (2) actinomycin D treatment also eliminated this MA staining (Fig. 7A), and (3) no in situ signal for *Hro-hes* was detected before first mitosis, other than a background staining of teloplasm also seen in controls (data not shown). The simplest interpretation of these results, that *Hro-hes* transcripts appear at the first mitosis, is also consistent with the finding that HRO-HES immunostaining labels nuclei at the two-cell stage, but not the one-cell stage (Fig. 5A). Alternatively, it could be that: (1) *Hro-hes* transcripts are present in the cytoplasm of the zygote but too diffusely distributed to be detected until they are localized to the MA during mitosis; (2) transcription is required for the synthesis of molecules that localize preexisting *Hro-hes* transcripts to the mitotic apparatus during mitosis, and (3) expression of HRO-HES is regulated posttranscriptionally, beginning at the two-cell stage.

To investigate this alternative, we undertook an RT-PCR analysis of *Hro-hes* expression using single embryos at selected time points during the first cell cycle, taking advantage of the fact that there is only one nuclear assembly per embryo during this time. Individual zygotes were staged relative to the time of emergence of the second polar body (approximately 100 min AZD). To increase the sensitivity of the method and to confirm the identity of the amplified bands, the resultant gels were blotted and hybridized with a ^{32}P-labeled *Hro-hes* probe. The probe was designed to correspond to a fragment internal to the primers used for

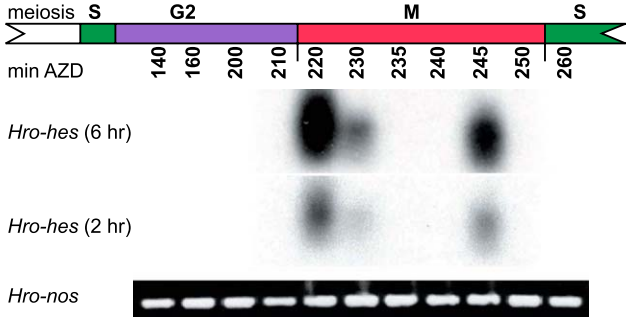

Fig. 8. *Hro-hes* is transcribed during mitosis: single cell RT-PCR/Southern analysis. Individual embryos were staged to within ±5 min and lysed for RT at indicated time points [minutes after zygote deposition (min AZD); the time line is not linear] during the first cell cycle (see Materials and methods for details). The corresponding cell cycle phases are indicated by the colored bar. The resultant gel was blotted and probed with a ^{32}P-labeled *Hro-hes* probe; the next two rows show 6- and 2-h exposures of the southern blot. As a control for the RT reaction, PCR for cDNAs derived from abundant maternal *Hro-nos* transcripts was carried out on the same set of RT samples (bottom row).

the RT-PCR (see Materials and methods for details). The Southern blot revealed bands of the expected size at three of the six time points sampled during mitosis and at none of the five points sampled during interphase (Fig. 8). Investigating the interesting possibility that *Hro-hes* transcription is further restricted to certain phases of mitosis requires further refinement of the protocol and is beyond the scope of the present work.

The central conclusion of these experiments is that *Hro-hes* mRNA is transcribed and accumulates during the first zygotic mitosis in *Helobdella*. These results do not preclude the possibility that *Hro-hes* is being transcribed before mitosis; but if so, the transcripts must be broken down so rapidly as to be undetectable even by the highly sensitive combination of RT-PCR and Southern blot analysis employed here. We cannot extend the RT-PCR/Southern analysis to multicellular stages of development because cell cycles in *Helobdella* are asynchronous beginning with the two-cell stage. Given the similar in situ patterns at the different stages, however, and the similar results with actinomycin D treatment, it seems likely that mitotic transcription of *Hro-hes* is occurring at later stages as well. This pattern of expression has not been observed for any of the *hes*-class genes characterized in vertebrates, arthropods or nematodes.

Discussion

Hro-hes is transcribed during mitosis and transcripts localize to the MA

We report here the first characterization of an *hes*-class gene from a segmented lophotrochozoan, the glossiphoniid leech *H. robusta*. The peak of *Hro-hes* transcript accumulation coincides with the production of segmental founder cells (blast cells) by embryonic stem cells (teloblasts), but *Hro-hes* is also expressed in teloblast precursors and non-segmental lineages throughout early development. *Hro-hes* is expressed in the teloblasts and primary blast cells of all five segmental lineages (M, N, O, P and Q). No striped pattern suggestive of a pair-rule function was observed for the expression of either *Hro-hes* or HRO-HES.

In situ hybridization also revealed that *Hro-hes* transcripts are associated with the MA of dividing cells, beginning with the first zygotic cell division. We have previously found a similar distribution of transcripts for an *eve*-class gene in *Helobdella* (Song et al., 2002). Curiously, transcripts for an *eve*-class gene were found to be localized to the centrosomes during the micromere-forming cleavages of another spiral cleaver, the snail *Ilyanassa obsoleta* (Lambert and Nagy, 2002). Both *Helobdella* (phylum Annelida) and *Ilyanassa* (phylum Mollusca) are grouped in the superphylum Lophotrochozoa. No such transcript localizations have been observed for either *hes*- or *eve*-class genes in arthropods or nematodes (superphylum Ecdysozoa) or vertebrates (superphylum Deuterostomia). *Hro-eve* is also expressed in a subset of developing neurons during stages 9–10, but the expression of *Hro-hes* has not yet been characterized at the cellular level for these stages.

Subcellular localization of mRNAs has been reported for many genes and is usually linked with translational regulation of the mRNA (reviewed by Kloc and Etkin, 1994). Of particular relevance to our results is the finding that *Xbub3* and *cyclinB1* mRNAs are localized to the MA of *Xenopus* embryos during cleavage; both transcripts contain cytoplasmic polyadenylation elements (CPEs) within their 3′-UTRs and their translation is regulated by CPE binding protein (CPEB) and maskin, both of which are located on the MA (Groisman et al., 2000). We note that both *Hro-hes* and *Hro-eve* contain putative CPEs within their 3′-UTRs; we speculate that the translation of these genes may be similarly controlled. The association of *Hro-hes* mRNA with the MA of dividing cells suggested that this gene might be transcribed during mitosis. The sensitivity of this in situ staining to actinomycin D supported this interpretation, and RT-PCR/Southern analysis of individual zygotes provides definitive evidence that *Hro-hes* is transcribed during the first mitosis. Mitotic transcription is unexpected but not without precedent. Of the approximately 6220 ORFs in yeast, approximately 55–195 are identified as being transcribed during mitosis (Krebs et al., 2000; Spellman et al., 1998).

Antiphasic oscillation of Hro-hes transcription and nuclear HRO-HES levels

In contrast to the case for *Hro-hes* transcripts, the immunohistochemical signal for HRO-HES protein is strongest in the nucleus during interphase and declines during mitosis. This could reflect dilution into cytoplasm following nuclear breakdown, protein turnover and/or masking of HRO-HES during mitosis. Whatever the cause, this means that *Hro-hes* transcription and HRO-HES nuclear protein levels cycle antiphasically in strict correlation with the cell cycle during cleavage, during the stem cell divisions by which teloblasts produce segmental founder cells (blast cells) and during the initial divisions leading from blast cells to definitive segmental tissues in *Helobdella*.

One interpretation of these observations is that *Hro-hes* transcription and HRO-HES protein localization are regulated by the cell cycle, independently of each other. By analogy with other systems, a more likely possibility is that HRO-HES represses *Hro-hes* transcription, either directly or indirectly. Repression by Hairy and other HES-class proteins has been clearly demonstrated (Barolo and Levine, 1997; Takebayashi et al., 1994); aspects of HES repression are mediated by binding a Groucho-class co-repressor to the C-terminal WRPW domain (Fisher et al., 1996) and also by interacting with the SIR2-class of histone deacetylase (Rosenberg and Parkhurst, 2002). In addition, autoinhibition of mammalian *hes1* transcription by binding of HES1 protein to its own promoter has been shown (Takebayashi

et al., 1994) and an oscillating antiphasic expression of *hes1* transcripts and HES1 protein has been demonstrated in serum-stimulated cells in culture; these oscillations also require the turnover of HES1 via the ubiquitinylation pathway (Hirata et al., 2002). These authors have also presented evidence that such autoinhibition functions in regulating *hes1* transcription in mouse, apparently contrary to previous conclusions for mouse (Jouve et al., 2000) and chick (Palmeirim et al., 1997). Our observations of antiphasically oscillating *Hro-hes* transcription and nuclear HRO-HES protein lead us to speculate that *Hro-hes* expression is regulated in part by autoinhibition, in tight conjunction with the cell cycle.

Evolution of segmentation

In recent years, three hypotheses have been offered to explain the relationship between segmentation in annelids, arthropods and vertebrates. The "Articulata hypothesis" originated with classical, character-based phylogenies; it holds that annelids and arthropods have evolved from a common segmented ancestor and that segmentation arose independently in chordates (Cuvier, 1817; reviewed by Scholtz, 2002). In contrast, the current consensus of molecular phylogenies holds that modern bilaterian animals represent three ancient clades (superphyla Deuterostomia, Ecdysozoa and Lophotrochozoa). If this is true, parsimony dictates that segmentation has evolved independently in annelids, arthropods and vertebrates because segmented phyla are a distinct minority in each clade (Brusca and Brusca, 1990). Finally, similarities between the expression patterns of *engrailed*- and *hes*-class genes in arthropods (Ecdysozoa) and chordates (Deuterostomia) have led some to propose that the last common ancestor of all three major groups was already segmented (De Robertis, 1997; Holland et al., 1997; Kimmel, 1996; Palmeirim et al., 1997).

Segmental structures arise sequentially in anteroposterior progression in most vertebrates, annelids and arthropods. As noted above, *hes*-class genes are expressed in the posterior growth zone of arthropods (Damen et al., 2000) and in the PSM of vertebrates (Bessho et al., 2001; Hirata et al., 2002; Holley et al., 2000; Jouve et al., 2000; Muller et al., 1996; Oates and Ho, 2002; Palmeirim et al., 1997; Pourquie, 2001a,b). Here, we have shown that an *hes*-class gene is also expressed in the posterior growth zone (i.e., the teloblasts and blast cells) of *H. robusta*, representing the third major group of segmented animals. We speculate that *Hro-hes* is part of a molecular network that operates under the control of the cell cycle and regulates cell fate decisions during cleavage and segmentation in the early *Helobdella* embryo.

However, we do not believe our results necessarily support the hypothesis of a segmented common ancestor for bilaterians, or even among the protostomes. Another scenario is that: (1) stem cells (a prominent feature of basally branched groups such as Porifera and Cnidaria) were a feature of the urbilaterian and that segmentation has arisen independently in a minority of modern phyla; (2) the inherent periodicity of gene expression and cell fate decisions associated with ancestral stem cell processes were modified in various ways during evolution to generate the repeating definitive structures we identify as segments in adult animals; (3) *hes*-class genes were involved in ancestral stem cell cycle and cell fate decisions and have been retained in all three of the major groups; (4) *hes* genes have acquired distinct roles during the independent evolution of segmentation in vertebrates, annelids and arthropods.

Thus, we propose that the stem cell populations in the ancestor bilaterian had properties that were modified to generate overt segmentation independently in a minority of taxa in the three major descendant groups. A prediction of this model is that genes involved in ancestral stem cell processes should be present in both segmented and unsegmented animals. We note that the *hes*-class gene (*lin-22*) exhibits a role in the A–P body pattern by regulating stem cell differentiation in the unsegmented nematode (Wrischnik and Kenyon, 1997). In this regard, it will be of interest to determine if *hes*-class genes are expressed in stem cells of other unsegmented taxa.

Acknowledgments

This work was supported by NIH Grant RO1 GM 60240 to DAW. CyclinA plasmid was kindly provided by Shirley T. Bissen.

References

Adoutte, A., Balavoine, G., Lartillot, N., Lespinet, O., Prud'homme, B., de Rosa, R., 2000. The new animal phylogeny: reliability and implications. Proc. Natl. Acad. Sci. U. S. A. 97, 4453–4456.

Aguinaldo, A.M., Turbeville, J.M., Linford, L.S., Rivera, M.C., Garey, J.R., Raff, R.A., Lake, J.A., 1997. Evidence for a clade of nematodes, arthropods and other moulting animals. Nature 387, 489–493.

Aronson, B.D., Fisher, A.L., Blechman, K., Caudy, M., Gergen, J.P., 1997. Groucho-dependent and -independent repression activities of Runt domain proteins. Mol. Cell. Biol. 17, 5581–5587.

Barolo, S., Levine, M., 1997. Hairy mediates dominant repression in the *Drosophila* embryo. EMBO J. 16, 2883–2891.

Bessho, Y., Sakata, R., Komatsu, S., Shiota, K., Yamada, S., Kageyama, R., 2001. Dynamic expression and essential functions of Hes7 in somite segmentation. Genes Dev. 15, 2642–2647.

Bier, E., Vaessin, H., Younger-Shepherd, S., Jan, L.Y., Jan, Y.N., 1992. Deadpan, an essential pan-neural gene in *Drosophila*, encodes a helix-loop-helix protein similar to the hairy gene product. Genes Dev. 6, 2137–2151.

Bissen, S.T., Weisblat, D.A., 1987. Early differences between alternate n blast cells in leech embryo. J. Neurobiol. 18, 251–270.

Bissen, S.T., Weisblat, D.A., 1989. The durations and compositions of cell cycles in embryos of the leech, *Helobdella triserialis*. Development 106, 105–118.

Brusca, R.C., Brusca, G.J., 1990. Invertebrates. Sinauer Assoc., Sunderland.

Carroll, S.B., Laughon, A., Thalley, B.S., 1988. Expression, function, and regulation of the hairy segmentation protein in the *Drosophila* embryo. Genes Dev. 2, 883–890.

Collins, A.G., Valentine, J.W., 2001. Defining phyla: evolutionary pathways to metazoan body plans. Evol. Dev. 3, 432–442.

Cuvier, G., 1817. Le règne animal. Déterville, Paris.

Damen, W., Weller, M., Tautz, D., 2000. Expression patterns of hairy, even-skipped, and runt in the spider *Cupiennius salei* imply that these genes were segmentation genes in a basal arthropod. Proc. Natl. Acad. Sci. U. S. A. 97, 4515–4519.

Dawson, S.R., Turner, D.L., Weintraub, H., Parkhurst, S.M., 1995. Specificity for the hairy/enhancer of split basic helix-loop-helix (bHLH) proteins maps outside the bHLH domain and suggests two separable modes of transcriptional repression. Mol. Cell. Biol. 15, 6923–6931.

De Robertis, E.M., 1997. Evolutionary biology. The ancestry of segmentation. Nature 387, 25–26.

Desjeux, I., Price, D.J., 1999. The production and elimination of supernumerary blast cells in the leech embryo. Dev. Genes Evol. 209, 284–293.

Feder, J.N., Jan, L.Y., Jan, Y.N., 1993. A rat gene with sequence homology to the *Drosophila* gene hairy is rapidly induced by growth factors known to influence neuronal differentiation. Mol. Biol. Cell 13, 105–113.

Feder, J.N., Li, L., Jan, L.Y., Jan, Y.N., 1994. Genomic cloning and chromosomal localization of HRY, the human homolog to the *Drosophila* segmentation gene, hairy. Genomics 20, 56–61.

Fisher, A.L., Ohsako, S., Caudy, M., 1996. The WRPW motif of the hairy-related basic helix-loop-helix repressor proteins acts as a 4-amino-acid transcription repression and protein-protein interaction domain. Mol. Biol. Cell 16, 2670–2677.

Goldstein, B., Leviten, M.W., Weisblat, D.A., 2001. Dorsal and snail homologs in leech development. Dev. Genes Evol. 211, 329–337.

Groisman, I., Huang, Y.S., Mendez, R., Cao, Q., Theurkauf, W., Richter, J.D., 2000. CPEB, maskin, and cyclin B1 mRNA at the mitotic apparatus: implications for local translational control of cell division. Cell 103, 435–447.

Hirata, H., Yoshiura, S., Ohtsuka, T., Bessho, Y., Harada, T., Yoshikawa, K., Kageyama, R., 2002. Oscillatory expression of the bHLH factor Hes1 regulated by a negative feedback loop. Science 298, 840–843.

Holland, L.Z., Kene, M., Williams, N.A., Holland, N.D., 1997. Sequence and embryonic expression of the amphioxus engrailed gene (AmphiEn): the metameric pattern of transcription resembles that of its segment-polarity homolog in *Drosophila*. Development 124, 1723–1732.

Holley, S.A., Geisler, R., Nusslein-Volhard, C., 2000. Control of her1 expression during zebrafish somitogenesis by a delta-dependent oscillator and an independent wave-front activity. Genes Dev. 14, 1678–1690.

Hooper, K.L., Parkhurst, S.M., Ish-Horowicz, D., 1989. Spatial control of hairy protein expression during embryogenesis. Development 107, 489–504.

Huang, F.Z., Kang, D., Ramirez-Weber, F.A., Bissen, S.T., Weisblat, D.A., 2002. Micromere lineages in the glossiphoniid leech *Helobdella*. Development 129, 719–732.

Ingham, P.W., 1985. Genetic control of the spatial pattern of selector gene expression in *Drosophila*. Cold Spring Harbor Symp. Quant. Biol. 50, 201–208.

Jouve, C., Palmeirim, I., Henrique, D., Beckers, J., Gossler, A., Ish-Horowicz, D., Pourquie, O., 2000. Notch signalling is required for cyclic expression of the hairy-like gene HES1 in the presomitic mesoderm. Development 127, 1421–1429.

Kang, D., Pilon, M., Weisblat, D.A., 2002. Maternal and zygotic expression of a nanos-class gene in the leech *Helobdella robusta*: primordial germ cells arise from segmental mesoderm. Dev. Biol. 245, 28–41.

Kimmel, C.B., 1996. Was Urbilateria segmented? Trends Genet. 12, 329–331.

Kloc, M., Etkin, L.D., 1994. Delocalization of Vg1 mRNA from the vegetal cortex in *Xenopus* oocytes after destruction of Xlsirt RNA. Science 265, 1101–1103.

Knust, E., Bremer, K.A., Vassin, H., Ziemer, A., Tepass, U., Campos-Ortega, J.A., 1987. The enhancer of split locus and neurogenesis in *Drosophila melanogaster*. Dev. Biol. 122, 262–273.

Krebs, J.E., Fry, C.J., Samuels, M.L., Peterson, C.L., 2000. Global role for chromatin remodeling enzymes in mitotic gene expression. Cell 102, 587–598.

Lambert, J.D., Nagy, L.M., 2002. Asymmetric inheritance of centrosomally localized mRNAs during embryonic cleavages. Nature 420, 682–686.

Muller, M., Weizsacker, E., Campos-Ortega, J.A., 1996. Expression domains of a zebrafish homologue of the *Drosophila* pair-rule gene hairy correspond to primordia of alternating somites. Development 122, 2071–2078.

Nusslein-Volhard, C., Wieschaus, E., 1980. Mutations affecting segment number and polarity in *Drosophila*. Nature 287, 795–801.

Lewis, J., 2003. Autoinhibition with transcriptional delay: a simple mechanism for the zebrafish somitogenesis oscillator. Curr. Biol. 13, 1398–1408.

Oates, A.C., Ho, R.K., 2002. Hairy/E(spl)-related (Her) genes are central components of the segmentation oscillator and display redundancy with the Delta/Notch signaling pathway in the formation of anterior segmental boundaries in the zebrafish. Development 129, 2929–2946.

Ohsako, S., Hyer, J., Panganiban, G., Oliver, I., Caudy, M., 1994. Hairy function as a DNA-binding helix-loop-helix repressor of *Drosophila* sensory organ formation. Genes Dev. 8, 2743–2755.

Palmeirim, I., Henrique, D., Ish-Horowicz, D., Pourquie, O., 1997. Avian hairy gene expression identifies a molecular clock linked to vertebrate segmentation and somitogenesis. Cell 91, 639–648.

Pilon, M., Weisblat, D.A., 1997. A nanos homolog in leech. Development 124, 1771–1780.

Pourquie, O., 2001a. The vertebrate segmentation clock. J. Anat. 199, 169–175.

Pourquie, O., 2001b. Vertebrate somitogenesis. Annu. Rev. Cell Dev. Biol. 17, 311–350.

Rosenberg, M.I., Parkhurst, S.M., 2002. *Drosophila* Sir2 is required for heterochromatic silencing and by euchromatic Hairy/E(Spl) bHLH repressors in segmentation and sex determination. Cell 109, 447–458.

Ruiz-Trillo, I., Riutort, M., Littlewood, D.T., Herniou, E.A., Baguna, J., 1999. Acoel flatworms: earliest extant bilaterian Metazoans, not members of Platyhelminthes. Science 283, 1919–1923.

Rushlow, C.A., Hogan, A., Pinchin, S.M., Howe, K.M., Lardelli, M., Ish-Horowicz, D., 1989. The *Drosophila hairy* protein acts in both segmentation and bristle patterning and shows homology to N-myc. EMBO J. 8, 3095–3103.

Ryskov, A.P., Ivanov, P.L., Kramerov, D.A., Georgiev, G.P., 1983. Mouse ubiquitous B2 repeat in polysomal and cytoplasmic poly(A)+RNAs: unidirectional orientation and 3′-end localization. Nucleic Acids Res. 11, 6541–6558.

Sambrook, J., Maniatis, T., Fritsch, E.F., 1989. Molecular Cloning: A Laboratory Manual. Cold Spring Harbor Laboratory, Cold Spring Harbor, NY.

Scholtz, G., 2002. The Articulata hypothesis—Or what is a segment? Org. Divers. Evol. 2, 197–215.

Shankland, M., 1999. Anteroposterior pattern formation in the leech embryo. In: Moody, S.A. (Ed.), Cell Lineage and Fate Determination. Academic Press, San Diego, pp. 207–224.

Smith, C.M., Weisblat, D.A., 1994. Micromere fate maps in leech embryos: lineage-specific differences in rates of cell proliferation. Development 120, 3427–3438.

Sommer, R.J., Tautz, D., 1993. Involvement of an orthologue of the *Drosophila* pair-rule gene hairy in segment formation of the short germ-band embryo of *Tribolium* (Coleoptera). Nature 361, 448–450.

Song, M.H., Huang, F.Z., Chang, G.Y., Weisblat, D.A., 2002. Expression and function of an even-skipped homolog in the leech *Helobdella robusta*. Development 129, 3681–3692.

Spellman, P.T., Sherlock, G., Zhang, M.Q., Iyer, V.R., Anders, K., Eisen, M.B., Brown, P.O., Botstein, D., Futcher, B., 1998. Comprehensive identification of cell cycle-regulated genes of the yeast *Sac-*

charomyces cerevisiae by microarray hybridization. Mol. Biol. Cell 9, 3273–3297.

Spencer, W.E., Christensen, M.J., 1999. Multiplex relative RT-PCR method for verification of differential gene expression. Biotechniques 27, 1044–1046, 1048–1052.

Takebayashi, K., Sasai, Y., Sakai, Y., Watanabe, T., Nakanishi, S., Kageyama, R., 1994. Structure, chromosomal locus, and promoter analysis of the gene encoding the mouse helix-loop-helix factor HES-1. Negative autoregulation through the multiple N box elements. J. Biol. Chem. 269, 5150–5156.

Weisblat, D.A., Huang, F.Z., 2001. An overview of glossiphoniid leech development. Can. J. Zool. 79, 218–232.

Weisblat, D.A., Kim, S.Y., Stent, G.S., 1984. Embryonic origins of cells in the leech *Helobdella triserialis*. Dev. Biol. 104, 65–85.

Wrischnik, L.A., Kenyon, C.J., 1997. The role of lin-22, a hairy/enhancer of split homolog, in patterning the peripheral nervous system of *C. elegans*. Development 124, 2875–2888.

Zackson, S.L., 1984. Cell lineage, cell–cell interaction, and segment formation in the ectoderm of a glossiphoniid leech embryo. Dev. Biol. 104, 143–160.